Journal of Pharmaceutical and Biomedical Analysis 56 (2011) 336–342

Contents lists available at ScienceDirect

Journal of Pharmaceutical and Biomedical Analysis

journal homepage: www.elsevier.com/locate/jpba

Binding studies of phloridzin with human serum albumin and its effect on the conformation of protein

Yuanyuan Yue[a,*], Jianming Liu[a], Jing Fan[a], Xiaojun Yao[b]

[a] School of Chemistry and Environmental Science, Henan Normal University, Xinxiang, Henan 453007, PR China
[b] Department of Chemistry, Lanzhou University, Lanzhou, Gansu 730000, PR China

ARTICLE INFO

Article history:
Received 24 January 2011
Received in revised form 2 May 2011
Accepted 15 May 2011
Available online 20 May 2011

Keywords:
Phloridzin
Human serum albumin (HSA)
Three-dimensional (3D) fluorescence
Fourier transformation infrared spectra (FT-IR)
Molecular modeling

ABSTRACT

In this study, the binding mode of phloridzin with human serum albumin (HSA) was established under physiological condition. The binding study is important to understand the pharmacokinetics and toxicity of phloridzin. The results proved the mechanism of fluorescence quenching of HSA by phloridzin was due to the formation of HSA–phloridzin complex. The binding constants, the number of binding sites and thermodynamic parameters were calculated. In addition, the alterations of HSA secondary structure in the presence of phloridzin were confirmed by the evidences from Fourier transform infrared (FT-IR), UV–visible absorption, circular dichroism (CD), synchronous and three-dimensional fluorescence spectroscopy. Alterations of protein conformation were observed with reduction of α-helix from 54% (free HSA) to 50% in the HSA–phloridzin complexes, indicating a partial protein unfolding. The distance between phloridzin and HSA was 3.74 nm according to fluorescence resonance energy transfer theory. In addition, the effects of common ions on the constants of HSA–phloridzin complex were also discussed.

1. Introduction

Phloridzin (Fig. 1) is a dihydrochalcone typically contained in apples. The main biological effect of phloridzin is its competitive inhibition of intestinal glucose uptake *via* sodium D-glucose cotransporter 1 (SGLT1), which is considered to be antidiabetic compounds [1,2]. It has also been proved that phloridzin was effective in preventing bone resorption in an ovariectomized rat model with chronic inflammation due to its phytoestrogenic, antioxidant and anti-inflammatory activities [3]. In recent years, phloridzin has been widely used in human medicine. Phlorizin is also a naturally occurring constituent of the human diet, because apple juice [4] and apple fruit [5] have been shown to contain phlorizin. In consideration of the possible pharmaceutical benefit of phlorizin and exist in our diet, it leads us to investigate the interaction of phloridzin with protein.

Of all the proteins, human serum albumin (HSA) is found the most abundant protein in blood plasma [6,7]. It is principally characterized by its remarkable ability to bind and transport a variety of endogenous and exogenous ligands such as drugs and chemical contaminants [8–11]. The absorption, distribution, metabolism, and excretion properties as well as the stability and toxicity of drugs can be significantly affected as a result of their binding to serum albumins [12]. Studies showed the conformational changes of proteins induced by its interaction with drugs, which may affect protein's biological function. Consequently, knowledge of interaction mechanisms between drugs and protein is of crucial importance for us to understand the pharmacodynamics and pharmacokinetics of a drug. The interaction can also influence the drug stability and toxicity during the chemotherapeutic process [13].

In this work, we used fluorescence spectroscopy, synchronous fluorescence (SF), and three dimensional (3D), circular dichroism (CD), FT-IR techniques to explore the pharmacological effects of phloridzin on HSA under simulative physiological conditions. The binding sites, modes, and forces were investigated for phloridzin binding to HSA and the secondary structure transition of HSA. Besides, the binding site of phloridzin to HSA was also discussed using automated molecular docking approach. In addition, the effect of common ions on the binding constant of HSA–phloridzin was examined.

2. Materials and methods

2.1. Materials

HSA (fatty acid free < 0.05%) was purchased from Sigma–Aldrich (St. Louis, MO, USA) and dissolved in Tris–HCl buffer of pH = 7.4 containing 0.1 M NaCl to form a 3.0×10^{-5} M solution and then stored at 0–4 °C. Phloridzin was purchased from Sigma-Aldrich. Double-distilled water was used throughout experiments. The

* Corresponding author. Tel.: +86 373 3325386; fax: +86 373 3325336.
E-mail address: yuanyuanyue@htu.cn (Y. Yue).

0731-7085/$ – see front matter © 2011 Elsevier B.V. All rights reserved.
doi:10.1016/j.jpba.2011.05.018

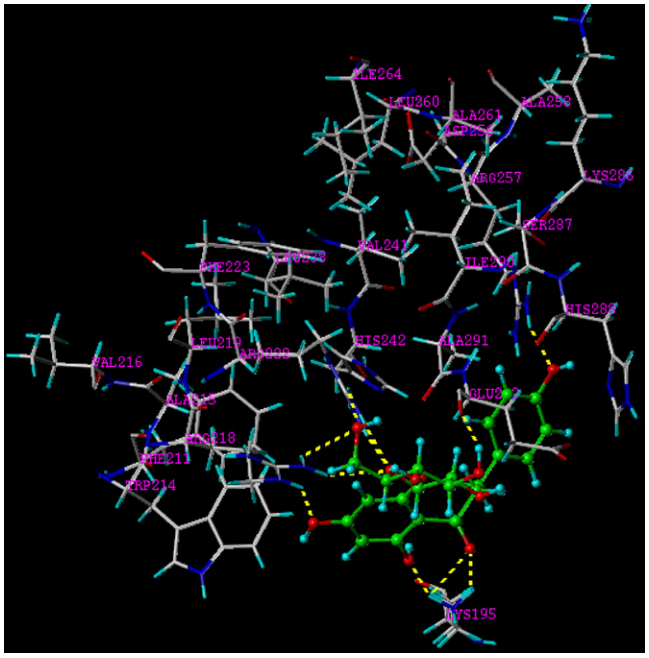

Fig. 1. Molecular modeling of phloridzin bound HSA (only residues around 6.5 Å of phloridzin was displayed). The residues of HSA are represented using gray ball and stick model and the phloridzin structure is represented by a green one. The hydrogen bond between phloridzin and HSA is represented using yellow dashed line. (For interpretation of the references to color in this figure legend, the reader is referred to the web version of the article.)

stock solution of phloridzin was prepared at concentration of 1.0×10^{-3} M. A pH-3 digital pH meter (Shanghai Lei Ci Device Works, Shanghai, China) was used with a combined glass electrode, which was calibrated with standard pH buffer solutions.

2.2. Apparatus and methods

The structure of HSA was downloaded from the Brookhaven Protein Data Bank (http://www.rcsb.org/pdb). The crystal structure of HSA (entry codes: 1H9Z) obtained by X-ray crystallography was used as a template and all water molecules were removed. Sybyl 6.9 [14] was used to generate the 3D structure of phloridzin and the energy minimized conformation was obtained with the help of the Tripos force field with Gasteiger-Marsili charges. The Lamarckian genetic algorithm (LGA) was applied to deal with the HSA–phloridzin interaction. FlexX program was applied to calculate the interaction mode between phloridzin and HSA. During the docking process, a maximum of 10 conformers were considered for the molecule. The conformer with the lowest binding free energy was used for further analysis. All calculations were performed on SGI FUEL workstation.

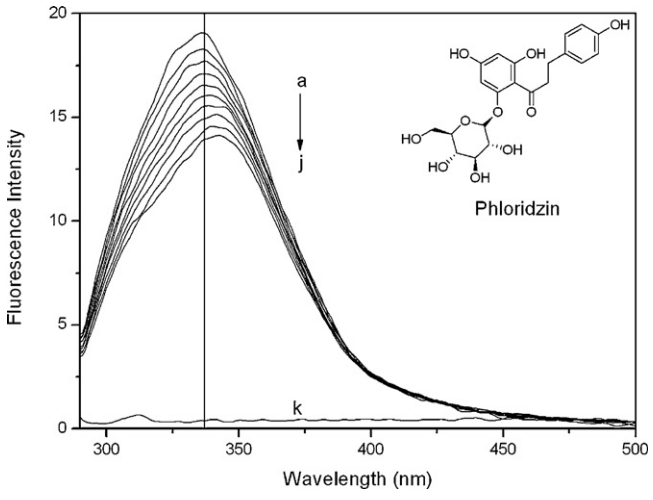

Fig. 2. Fluorescence spectra of the HSA at pH = 7.4 in the native state (a) and in the presence of 9.90, 19.60, 29.12, 38.46, 47.62, 56.60, 65.42, 74.07, 82.57 μM (b–j); 9.90 μM phloridzin only (k). T = 298 K.

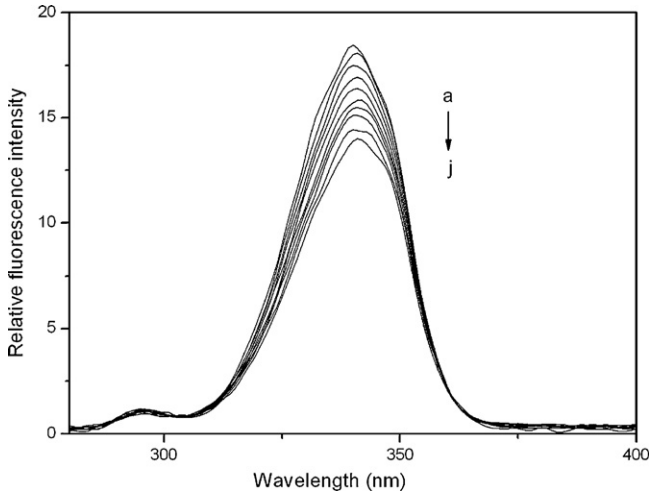

Fig. 3. Synchronous fluorescence spectrum of HSA in the absence and presence of phloridzin, $\Delta\lambda$ = 60. (a) 3.0 μM HSA; (b–j) 3.0 μM HSA in the presence of 9.90, 19.60, 29.12, 38.46, 47.62, 56.60, 65.42, 74.07, 82.57 μM phloridzin, respectively. pH = 7.40, T = 298 K.

All fluorescence measurements were carried out on a FP-6500 Fluorescence Spectrometer (JASCO, Japan) and 1 cm path-length quartz cell. The fluorescence emission spectra were recorded in the wavelength range 290–500 nm by exciting HSA at 280 nm using a slit width of 5 nm. The synchronous fluorescence spectra were recorded from 280 to 400 nm at $\Delta\lambda$ = 60 nm. The required temperature was maintained by a circulating water bath (Thermo/HAAKE DC30-K20, USA, ±0.01 °C accuracy).

UV absorption spectra were measured on UV-1700 PharmaSpec (Shimadzu, Japan) spectrophotometer with a 1-cm cuvette. UV absorption spectra were measured from 190 nm to 350 nm at room temperature.

CD spectra were recorded with a Jasco-810 spectropolarimeter (Jasco, Japan) using a 10 mm path length quartz cell. Three scans were averaged for each CD spectrum in the range 200–250 nm at 298 K. Spectra were corrected for buffer absorbance and recorded at the molar ratio HSA to drug of 1:2. The secondary structure content was calculated using follow equation [15]:

$$\alpha\text{-helix}\,\% = \left\{ \frac{-[\theta]_{208} - 4000}{33000 - 4000} \right\} \times 100 \quad (1)$$

Infrared spectra were recorded on a FT-IR spectrometer (a Tensor 27 FT-IR spectrometer, Bruker, German), equipped with deuterated triglycine sulfate (DTGS) detector and KBr beam splitter. First, the absorbance of buffer and free phloridzin solutions were recorded and digitally subtracted. Then the absorbance of phloridzin was subtracted from the spectra of HSA–phloridzin to get the FT-IR difference spectra of HSA. The standard of FT-IR subtraction was the spectrum between 2200 and 1800 cm^{-1} was a smooth straight [16]. These spectral differences were used to characterize the nature of the drug–protein interaction.

For three-dimensional fluorescence studies the spectra of samples were recorded range between 250 and 600 nm for λ_{ex}, λ_{em} was set between 220 and 360 nm with increment of 5 nm, the total number of scanning curves was 31.

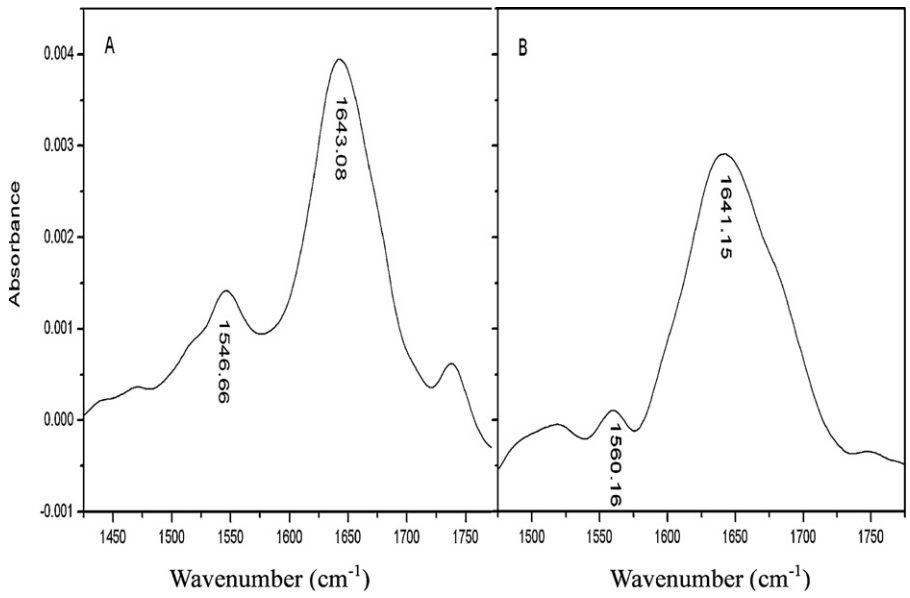

Fig. 4. FT-IR spectra and different spectra of HSA in aqueous solution: (a) FT-IR spectrum of HSA and (b) FT-IR difference spectrum of HSA obtained by subtracting the spectrum of the phloridzin-free form from that of the phloridzin–HSA form at 298 K. Tris–HCl buffer (pH = 7.40); C_{HSA} = 3.0 μM; $C_{phloridzin}$ = 6.0 μM. pH = 7.40.

The fluorescence spectra of phloridzin–HSA were recorded in presence and absence of various ions at 335 nm upon excitation at 280 nm. The concentrations of HSA and common ions (Zn^{2+}, Ni^{2+}, Mg^{2+}, Al^{3+}, Fe^{3+}) were fixed at 6.67 μM while the concentration of phloridzin was varied from 0.99 to 9.10×10^{-5} M.

3. Results and discussion

3.1. Identification of the specific binding sites on HSA

Descriptions of the 3-D structure of crystalline albumin have revealed that HSA is comprised of three structurally similar helical domains (I-III), each of which has two subdomains (A and B) [17]. Several binding studies have shown the principal regions of ligand binding are located in hydrophobic cavities in subdomains IIA and IIIA [18,19], the so-called site I and site II, respectively [20]. The sole tryptophan residue (Trp-214) of HSA is in subdomain IIA.

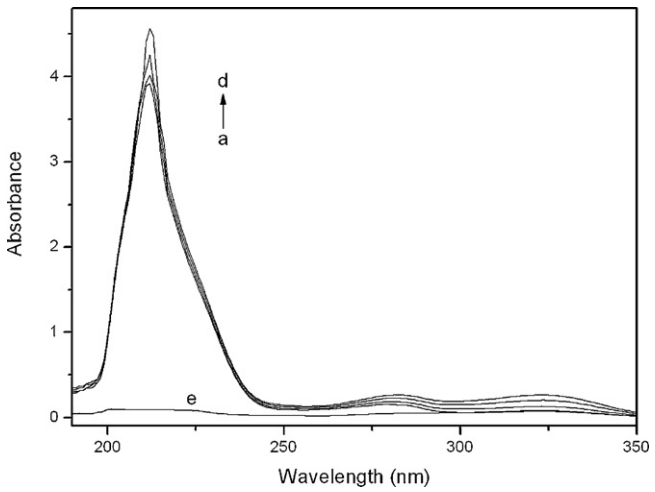

Fig. 5. UV-absorption spectra of free HSA (3 μM) and different concentrations of phloridzin (0.33, 0.67, 1.0×10^{-5} M) with HSA. Here, (a)–(d) are from free HSA to different concentrations of phloridzin. A concentration of 0.33×10^{-5} M phloridzin (e) was used for phloridzin only. pH = 7.40, T = 298 K.

In order to identify potential binding sites, HSA model was established with phloridzin. As shown in Fig. 1, the best energy ranked result between HSA and phloridzin was generated. The docking showed that phloridzin was located within the binding pocket of subdomain IIA of the protein (The Warfarin Binding Pocket), and adjacent to hydrophobic residues Ala-215, Leu-238, Trp-214, Val-216 of subdomain IIA of HSA. Thus, we can conclude that the interaction of phloridzin with HSA was mainly hydrophobic. We noted that the Trp-214 residue of HSA was in close proximity to the phloridzin and did not participate in phloridzin–HSA complexation, which provided a good structural basis to explain the efficient quenching of HSA fluorescence in the presence of phloridzin. Furthermore, there were hydrogen interactions between Arg-257, Lys-195, Arg-222, Arg-218 and phloridzin. These results indicated that the interaction between phloridzin and HSA presented in subdomain IIA (site I) and dominated by hydrophobic force, and there also existence of hydrogen bonds force. The calculated value for the Gibbs free energy of binding phloridzin to HSA was -13.87 kJ mol^{-1}. Spectral experiments between phloridzin and HSA were taken to validate the results of molecular modeling as follows.

3.2. Fluorescence quenching of HSA by phloridzin

Fluorescence spectroscopy is an appropriate method to determine the interaction between small molecules and biomacromolecules. It is proverbial that the fluorescence of HSA comes from the tyrosine, tryptophan, and phenylalanine residue. Fig. 2 showed the emission spectra of HSA in the presence of various concentrations of phloridzin. HSA showed a strong fluorescence emission with a peak at 335 nm at λ_{ex} = 280 nm. The phloridzin was almost non fluorescent or possess a very weak emission under the present experimental conditions. Increasing the concentration of phloridzin caused a progressive reduction of the fluorescence intensity and the maximum emission wavelength suffered a large red shift from 335 nm to 342 nm. These phenomena indicated the binding of phloridzin to HSA occurred and the interactions of HSA with phloridzin changed the environment of tryptophan, shifted to a more polar environment on ligand binding to HSA [21].

Table 1
Binding parameters and thermodynamic parameters for phloridzin–HSA system.

pH	T (K)	K ($\times 10^4$ M^{-1})	R^a	n	ΔG° (kJ mol^{-1})	ΔS° (J mol^{-1} K^{-1})	ΔH° (kJ mol^{-1})
7.4	289	6.67	0.9954	1.31	−26.73	70.30	−6.41
	296	6.45	0.9936	1.33	−27.22		
	303	6.12	0.9896	1.36	−27.71		
	310	5.56	0.9949	1.42	−28.20		

[a] R is the correlation coefficient.

3.3. Binding constants and the number of binding sites

According to the Scatchard equation [22], the fluorescence data were used to obtain the values of binding constant K

$$r/D_f = nK - rK \quad (2)$$

where r is the moles of small molecules bound per mole of protein, D_f is the molar concentration of free drug molecules, n is binding site multiplicity per class of binding site. The values of binding constant K and n were obtained from the Scatchard curves of phloridzin with HSA at different temperatures (289, 296, 303 and 310 K). The results were listed in Table 1.

Fluorescence quenching can be dynamic or static quenching. For dynamic, it resulted from collisional encounters between the fluorophore and the quencher; or static, resulting from the formation of a ground state complex between the fluorophore and the quencher. High temperatures tend to disrupt ground state complex formation. So a static quenching process will lead to a decrease in the quenching rate constant with raising temperature. The two forms of fluorescence quenching can be distinguished from each other by the differences in temperature-dependent behavior. The quenching rate constant of dynamic quenching will increase with raising temperature, because higher temperature leads to faster molecular diffusion. In contrast, the donor and acceptor molecules bind together to form a ground state complex, high temperatures tend to disrupt ground state complex formation, so a static quenching process will lead to a decrease in the quenching rate constant with raising temperature. In the Scatchard plots, straight lines were obtained, indicating phloridzin bound to a class of binding sites on HSA. It was seen that K decreased as the temperature increased (Table 1), indicating that the mechanism of the quenching might be a static quenching.

3.4. Binding determination of acting force

The acting forces between small molecules and biological macromolecules include hydrogen bonds, van der Waals interactions, electrostatic forces, and hydrophobic interaction forces. The signs and magnitudes of thermodynamic parameters for protein reactions can account for the main forces contributing to protein stability [23].

If the enthalpy change (ΔH°) does not vary significantly over the temperature range studied, then the values of the enthalpy change (ΔH°) as well as entropy change (ΔS°) can be determined from following equations (Eqs. (3) and (4)):

$$\Delta G^\circ = \Delta H^\circ - T\Delta S^\circ \quad (3)$$

$$\ln K_T = \frac{-\Delta H^\circ}{RT} + \frac{\Delta S^\circ}{R} \quad (4)$$

The values of K, ΔH°, ΔS° and ΔG° were summarized in Table 1. The negative values of ΔG° demonstrated the easy formation of phloridzin–HSA and it was an exothermic reaction. It was clear that phloridzin–HSA complexes were accompanied by negative enthalpy change (ΔH°) and positive entropy change (ΔS°), which indicated that the binding processes were exothermic and entropy driven. According to the rules summarized by Ross and Subramanian [24], for typical hydrophobic interactions, both ΔH° and ΔS° changes are positive, while negative ΔH° and ΔS° changes arise from the van der Waals force and hydrogen bonding formation in low dielectric media. Negative ΔH° value is also observed whenever there is hydrogen bonding in the binding. Therefore, both hydrophobic force and hydrogen bond interactions played a role in the binding reaction between phloridzin and HSA. Obviously, the above results were in good agreement with the information coming from molecular modeling. The experimental Gibbs free energy (296 K) was −27.22 kJ mol^{-1}, while −15.86 kJ mol^{-1} obtained by molecular docking study. Analyze the difference result might be that the X-ray structure of the protein from crystals differed from that the aqueous environment to which the HSA was exposed.

3.5. Conformation investigations

The synchronous fluorescence spectroscopy (SFS) technique was first introduced by Lloyd [25]. It was used to study the conformation change of protein. It means simultaneous scanning of the excitation and emission monochromators while maintaining a constant wavelength interval ($\Delta\lambda$) between them. The shift in the emission maximum reflects the changes of polarity around the chromophore molecule [26]. When $\Delta\lambda$ is maintained at 60 nm, the synchronous fluorescence of HSA is characteristic of tryptophan residue. Fig. 3 illustrated SFS of HSA progressively titrated with phloridzin by gradually increasing its concentration at pH = 7.40. It was observed that the emission wavelength of the tryptophan residues was a slight blue-shifted (~3 nm) in Fig. 3. It suggested that the interaction of phloridzin with HSA affected the conformation of tryptophan micro-area.

FTIR spectroscopy provides information about the secondary structure of proteins. Each compound has a characteristic of absorp-

Table 2
Three-dimensional fluorescence spectral characteristics of HSA and HSA–phloridzin system.

System		Peak a	Peak b
HSA	Peak position (E_x/E_m)	250/250–360/360	280/336
	Relative intensity (F)	9.84–66.22	18.55
HSA:phloridzin (1:2)	Peak position (E_x/E_m)	250/250–360/360	280/336
	Relative intensity (F)	9.18–63.00	16.34
HSA:phloridzin (1:4)	Peak position (E_x/E_m)	250/250–360/360	280/336
	Relative intensity (F)	5.99–59.83	15.48

Table 3
Effects of some common ions on HSA–phloridzin system.

System	Binding constant (M^{-1})	R^a
HSA + phloridzin	6.53×10^4	0.9987
HSA + phloridzin + Zn^{2+}	6.21×10^4	0.9921
HSA + phloridzin + Ni^{2+}	6.25×10^4	0.9924
HSA + phloridzin + Mg^{2+}	6.31×10^4	0.9879
HSA + phloridzin + Al^{3+}	6.06×10^4	0.9951
HSA + phloridzin + Fe^{3+}	6.17×10^4	0.9969

[a] R is the correlation coefficient for the K values.

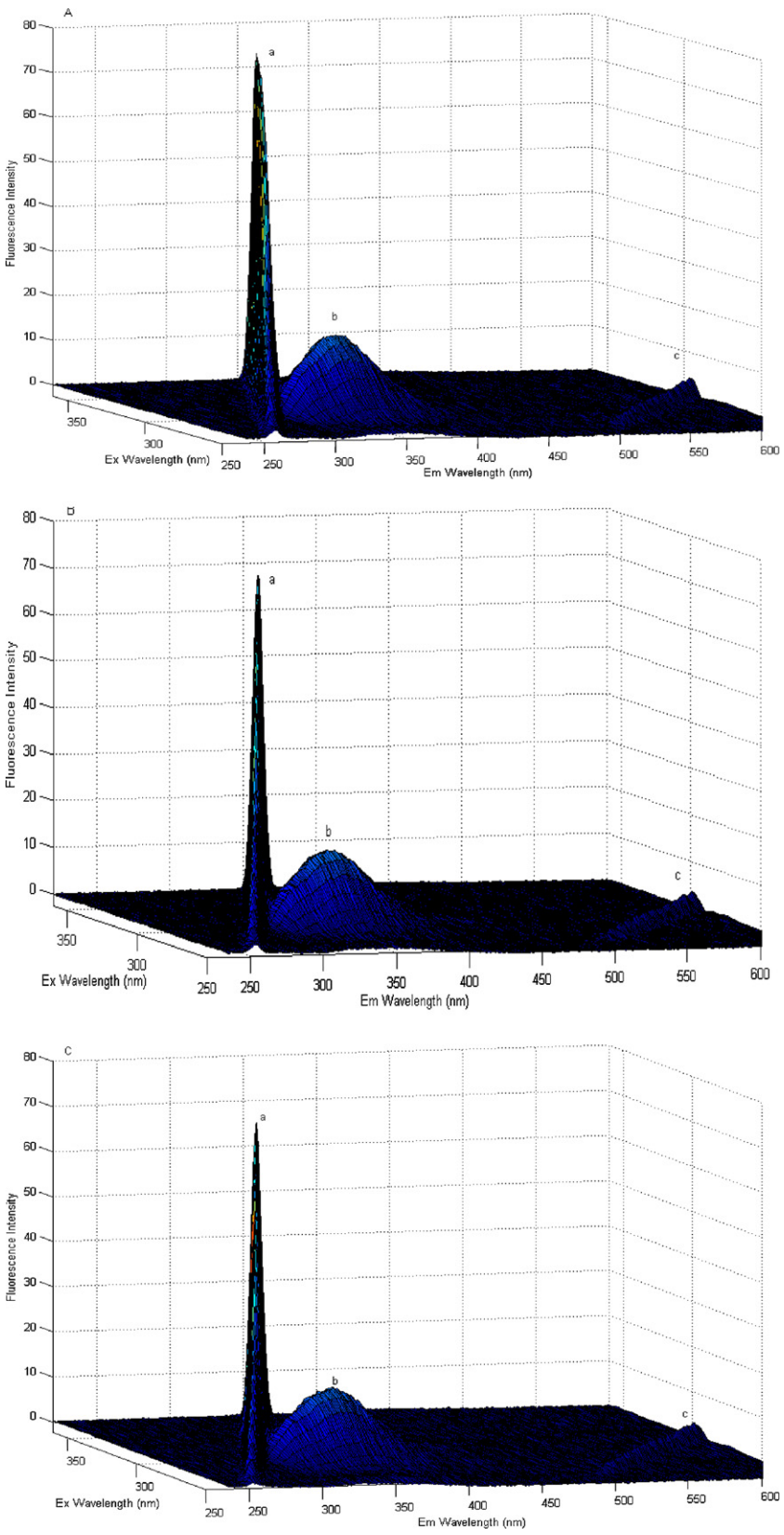

Fig. 6. Three-dimensional fluorescence spectra of HSA (A); HSA–phloridzin (1:2) (B); HSA–phloridzin (1:4) (C). $C_{(HSA)}$ = 3 μM. pH = 7.4, T = 298 K.

tion bands in its infrared spectrum. Characteristic bands found in the infrared spectra of proteins include the Amide I and Amide II. The absorption associated with the Amide I band (1600-1700 cm^{-1}) leads to stretching vibrations of the C=O bond of the amide, Amide II band (1500-1600 cm^{-1}) leads to bending vibrations of the N–H bond [27]. As shown in Fig. 4, the peak position of Amide I bands changed from 1643.08 to 1641.15 cm^{-1} and Amide II moved from 1546.66 to 1560.16 cm^{-1}, which indicated that the secondary struc-

ture of the protein had been changed after phloridzin was added. The possible reason was HSA–phloridzin complexes caused the rearrangement of the polypeptide carbonyl hydrogen bonding network. Consequently, the α-helical structure of protein was reduced.

To demonstrate the conformational changes of HSA induced by phloridzin, UV–vis absorption were used to monitor the changes in the secondary structure of protein. UV–vis absorption spectra of HSA with various amounts of phloridzin were obtained (Fig. 5). The absorption of HSA (about 210 nm) represents the content of α-helix structure of HSA [28]. As can be seen in Fig. 5, the fluorescence intensity of HSA was increased with the addition of phloridzin. Meanwhile, the formation of chromophore of phloridzin–HSA results in a little shift of phloridzin–HSA spectrum towards longer wavelength. The above two evidences clearly indicated the interaction between phloridzin and HSA, inducing the change of α-helix structure of protein [29].

Further experiments were carried out with circular dichroism to analyze the protein conformation. The CD spectrum of HSA have negative ellipticity at 208 and 222 nm, which were characteristic of an α-helix in the advanced structure of protein. The addition of phloridzin caused a little decrease in the band intensity at all sweep range of the CD without any significant shift of the peaks, which means the structure of HSA was also predominantly α-helical. The values of α-helix of HSA were calculated from Eq. (1). The α-helix content reduced from 54% to 50% at a molar ratio of HSA to phloridzin of 1:2. The drop off in the helical content was related with the fact that, as the phloridzin binds to the protein which led to a disordered structure with exposed hydrophobic residues and α-helix structure of HSA began unfolding [30,31].

The three-dimensional fluorescence spectra can provide total information regarding the fluorescence characteristics by changing excitation and emission wavelength simultaneously [32]. The 3D fluorescence spectra of HSA and HSA–phloridzin were shown in Fig. 6. Peak a was the rayleigh scattering peak ($\lambda_{ex} = \lambda_{em}$). Peak b mainly reflected the spectral behavior of tryptophan, and the maximum emission wavelength and the fluorescence intensity of the residue associated with its microenvironment's polarity. Peak c was the second-ordered scattering peak ($\lambda_{em} = 2\lambda_{ex}$). The changes of three dimension fluorescence spectra of HSA in the presence of different volume of phloridzin were listed in Table 2. It can be seen that the fluorescence intensity of peak a and b both decreased in the presence of phloridzin but to a different extent. We can conclude that the interaction of phloridzin with HSA increased the exposure of some hydrophobic regions which were previously buried. All these phenomena together with SF, FT-IR, UV–vis and CD spectra revealed that the binding of phloridzin to HSA induced conformational changes in HSA molecule.

3.6. Energy transfer between HSA and phloridzin

Nonradioactive energy transfer can be explained and determined by Förster's energy transfer theory. The theory is widely used to determine the distance between the amino acid residues and the drug in the binding site.

According to Förster's theory [33], the efficiency of energy transfer (E) by a FRET mechanism depends on the distance between donor and acceptor (r) as well as on Förster radius (R_0), at which 50% of the excitation energy is transferred to acceptor

$$E = 1 - \frac{F}{F_0} = \frac{R_0^6}{R_0^6 + r^6} \tag{5}$$

Then, R_0 is expressed using the following equation:

$$R_0^6 = 8.79 \times 10^{-25} K^2 N^{-4} \Phi J \tag{6}$$

where K^2 is the orientation factor related to the geometry of the donor–acceptor dipole, N is the refractive index of the medium, Φ expresses the donor's fluorescence quantum yield, and J stands for the degree of spectra overlap between the donor's emission and the acceptor's absorption. J can be calculated by Eq. (7):

$$J = \frac{\sum F(\lambda)\varepsilon(\lambda)\lambda^4 \Delta\lambda}{\sum F(\lambda)\Delta\lambda} \tag{7}$$

$F(\lambda)$ is the fluorescence intensity of the fluorescence donor when the wavelength is λ, $\varepsilon(\lambda)$ is the molar absorptivity coefficient of the receptor at wavelength of λ. We can evaluate J by overlapping spectrum of fluorescence spectrum of HSA and UV–visible spectrum of phloridzin. For HSA, the refractive index (N) of water is 1.36, $\Phi = 0.074$ [10], according to Eqs. (5)–(7), we could calculate that $J = 1.44 \times 10^{-14}$ cm^3 L mol^{-1}, $E = 0.062$ and $r = 3.74$ nm. The donor (tryptophan residues of the HSA) to acceptor (phloridzin) distance was less than 8 nm [34], indicating that the energy transfer from HSA to phloridzin occurred with high probability and the fluorescence quenching of HSA by phloridzin was also a non-radiation energy transfer process.

3.7. Influences of common ions on binding constant

Metal ions are vital to human body and play an essentially structural role in many proteins based coordinate bonds. In plasma, there are some metal ions, which can effect the reactions of the drugs and serum albumin. The effect of metal ions on the binding constants was investigated at 298 K and the results were summarized in Table 3. The lowered binding constant of phloridzin–HSA obtained in presence of common ions might be resulted from the competition between common ions and drug binding to the protein. Since such sites for the phloridzin and metal ion for HSA are not located in the same domain, there is no direct competition between phloridzin and the metal ions. So the K values of drug–HSA binding did not change considerably in the presence of divalent and trivalent metal ions. From the pharmacokinetics perspective, this will decrease the binding force between drug and HSA. Hence, more amount of phloridzin could be released in blood plasma [35]. High concentration of phloridzin in blood plasma will enhance the maximum effectiveness of the drug and may produce toxic effects.

4. Conclusions

In this paper, the interaction between phloridzin and HSA has been studied by fluorescence, SFS, CD, 3D, UV–vis and FT-IR spectroscopy. The investigation showed that phloridzin binding to HSA occurred *via* hydrophobic force and hydrogen bond interactions and caused a partial protein unfolding. Structural information regarding phloridzin binding mode and the effect of phloridzin–HSA complexation on the protein stability and secondary structure were also discussed. It was evident that unfolding of the protein with a significant decrease in the α-helix was observed upon complexation with the phloridzin. For docking and competition displacement experiments, it appeared that the binding site of phloridzin on the HSA was around site I. Thus, the study of this compound would be useful so as to understand the pharmaceutical agent to cure many diseases.

References

[1] J. Boyer, R.H. Liu, Apple phytochemicals and their health benefits, Nutr. J. 12 (2004) 3–5.
[2] J.R.L. Ehrenkranz, N.G. Lewis, C.R. Kahn, J. Roth, Phloridzin: a review, Diabetes Metab. Res. Rev. 21 (2005) 31–38.
[3] C. Puel, A. Quintin, J. Mathey, C. Obled, M.J. Davicco, P. Lebecque, S. Kati-Coulibaly, M.N. Horcajada, V. Coxam, Prevention of bone loss by phloridzin,

an apple polyphenol, in ovariectomized rats under inflammation condition, Calcif. Tissue Int. 77 (2005) 311–318.
[4] P.D. Bremner, C. Blacklock, G. Paganga, W. Mullen, C. Rice-Evans, A. Crozier, Comparison of the phenolic composition of fruit juices by single step gradient HPLC analysis of multiple chromatographic runs optimized for individual families, Free Radic. Res. 32 (2000) 549–559.
[5] A. Escarpa, M. Gonzalez, High-performance liquid chromatography with diode-array detection for the determination of phenolic compounds in peel and pulp from different apple varieties, J. Chromatogr. 823 (1998) 331–337.
[6] D.C. Carter, J.X. Ho, Structure of serum albumin, Adv. Protein Chem. 45 (1994) 153–203.
[7] Y.J. Hu, Y. Liu, X.H. Xiao, Investigation of the interaction between berberine and human serum albumin, Biomacromolecules 10 (2009) 517–521.
[8] J.C. D'eon, A.J. Simpson, R. Kumar, A.J. Baer, S.A. Mabury, Determining the molecular interactions of perfluorinated carboxylic acids with human sera and isolated human serum albumin using nuclear magnetic resonance spectroscopy, Environ. Toxicol. Chem. 29 (2010) 1678–1688.
[9] J.S. Mandeville, E. Froehlich, H.A. Tajmir-Riahi, Study of curcumin and genistein interactions with human serum albumin, J. Pharm. Biomed. Anal. 49 (2009) 468–474.
[10] E. Froehlich, J.S. Mandeville, C.J. Jennings, R. Sedaghat-Herati, H.A. Tajmir-Riahi, Dendrimers bind human serum albumin, J. Phys. Chem. B. 113 (2009) 6986–6993.
[11] C.N. N'soukpoe-Kossi, R. Sedaghat-Herati, C. Ragi, S. Hotchandani, H.A. Tajmir-Riahi, Retinol and retinoic acid bind human serum albumin: stability and structural features, Int. J. Biol. Macromol. 40 (2007) 484–490.
[12] R.E. Olson, D.D. Christ, Plasma protein binding of drugs, Annu. Rep. Med. Chem. 31 (1996) 327–336.
[13] P.N. Naik, S.A. Chimatadar, S.T. Nandibewoor, Interaction between a potent corticosteroid drug-Dexamethasone with bovine serum albumin and human serum albumin: a fluorescence quenching and Fourier transformation infrared spectroscopy study, J. Photochem. Photobiol. B. 100 (2010) 147–159.
[14] G. Morris, SYBYL Software, Version 6.9, Tripos Associates Inc., St. Louis, 2002.
[15] N. Greenlleld, D. Fastnan, Computed circular dichroism spectra for the evaluation of protein conformation, Biochemistry 8 (1969) 4108–4116.
[16] A.C. Dong, P. Huang, W.S. Caughey, Protein secondary structures in water from second-derivative amide I infrared spectra, Biochemistry 29 (1990) 3303–3308.
[17] X.M. He, D.C. Carter, Atomic structure and chemistry of human serum albumin, Nature 358 (1992) 209–215.
[18] S. Neelam, M. Gokara, B. Sudhamalla, D.G. Amooru, R. Subramanyam, Interaction studies of coumaroyltyramine with human serum albumin and its biological importance, J. Phys. Chem. B 114 (2010) 3005–3012.
[19] Q.L. Zhang, Y.N. Ni, S. Kokot, Molecular spectroscopic studies on the interaction between ractopamine and bovine serum albumin, J. Pharm. Biomed. 52 (2010) 280–288.
[20] J.R. Brown, Serum album: amino acid sequence, in: V.M. Rosenoer, M. Oratz, M.A. Rothschild (Eds.), Albumin Structure, Function and Uses, Pergamon Press, Oxford, 1977.
[21] D. Charbonneau, M. Beauregard, H.A. Tajmir-Riahi, J. Phys. Chem. 113 (2009) 1777–1784.
[22] G. Scatchard, The attractions of protein for small molecules and ions, Ann. N.Y. Acad. Sci. 51 (1949) 660–673.
[23] S.S. Kalanur, J. Seetharamappa, V.K.A. Kalalbandi, Characterization of interaction and the effect of carbamazepine on the structure of human serum albumin, J. Pharm. Biomed. 53 (2010) 660–666.
[24] P.D. Ross, S. Subramanian, Thermodynamics of protein association reactions: forces contributing to stability, Biochemistry 20 (1981) 3096–3102.
[25] J.B.F. Lloyd, Synchronized excitation of fluorescence emission spectra, Nature Phys. Sci. 231 (1971) 64–65.
[26] Y.Q. Wang, H.M. Zhang, G.C. Zhang, S.X. Liu, Q.H. Zhou, Z.H. Fei, Z.T. Liu, Studies of the interaction between paraquat and bovine hemoglobin, Int. J. Biol. Macromol. 41 (2007) 243–250.
[27] J.W. Brauner, C.R. Flach, R. Mendeisohn, A quantitative reconstruction of amide I contour in the IR spectra of globular protein: from structure to spectrum, J. Am. Chem. Soc. 127 (2005) 100–109.
[28] H.N. Hou, Z.D. Qi, Y.W. OuYang, F.L. Liao, Y. Zhang, Y. Liu, Studies on interaction between vitamin B12 and human serum albumin, J. Pharm. Biomed. 47 (2008) 134–139.
[29] W.Y. He, Y. Li, J.N. Tian, H.X. Liu, Z.D. Hu, X.G. Chen, Spectroscopic studies on binding of shikonin to human serum albumin, J. Photochem. Photobiol. A 174 (2005) 53–61.
[30] M.N. Jones, A theoritical approach to the binding of amphipatic molecules to globular proteins, Biochem. J. 151 (1975) 109–114.
[31] S. Ray, A. Chakrabarti, Erythroid spectrin in miceller detergents, Cell. Motil. Cytoskeleton 54 (2003) 16–28.
[32] M.J. Rodríguez-Cuesta, R. Boqué, F.X. Rius, D.P. Zamora, M.M. Galera, A.G. Frenich, Determination of carbendazim, fuberidazole and thiabendazole by threedimensional excitation–emission matrix fluorescence, Anal. Chim. Acta 491 (2003) 47–56.
[33] T. Förster, Modern Quantum Chemistry, vol. 3, Academic Press, New York, 1996, pp. 93–137.
[34] B. Valeur, J.C. Brochon, New Trends in Fluorescence Spectroscopy, 6th ed., Springer Press, Berlin, 1999, p. 25.
[35] G.C. Zhang, Y.Q. Wang, H.M. Zhang, S.H. Tang, W.H. Tao, Pestic. Biochem. Phys. 87 (2007) 23–29.